

PAID: A Framework of Product-Centric Advertising Image Design

Hongyu Chen*
yinchen.chy@alibaba-inc.com
Alibaba Group
Beijing, China

Min Zhou*
yunqi.zm@alibaba-inc.com
Alibaba Group
Beijing, China

Jing Jiang*[†]
jiangjing1998@bupt.edu.cn
Beijing University of Posts and
Telecommunications
Beijing, China

Jiale Chen
cjl414939@taobao.com
Alibaba Group
Beijing, China

Yang Lu
ly430273@alibaba-inc.com
Alibaba Group
Beijing, China

Bo Xiao
xiaobo@bupt.edu.cn
Beijing University of Posts and
Telecommunications
Beijing, China

Tiezheng Ge[‡]
tiezheng.gt@alibaba-inc.com
Alibaba Group
Beijing, China

Bo Zheng
bozheng@alibaba-inc.com
Alibaba Group
Beijing, China



Figure 1: Generated advertising images by our methods with a product foreground image, taglines, and a target size as input.

Abstract

Creating visually appealing advertising images is often a labor-intensive and time-consuming process. Is it possible to automatically generate such images using only basic product information—specifically, a product foreground image, taglines, and a target size? Existing methods mainly focus on parts of the problem and fail to provide a comprehensive solution. To address this gap, we propose a novel multistage framework called Product-Centric Advertising Image Design (PAID). It consists of four sequential

stages to highlight product foregrounds and taglines while achieving overall image aesthetics: prompt generation, layout generation, background image generation, and graphics rendering. Different expert models are designed and trained for the first three stages: First, we use a visual language model (VLM) to generate background prompts that match the products. Next, a VLM-based layout generation model arranges the placement of product foregrounds, graphic elements (taglines and decorative underlays), and various non-graphic elements (objects from the background prompt). Following this, we train an SDXL-based image generation model that can simultaneously accept prompts, layouts, and foreground controls. To support the PAID framework, we create corresponding datasets with over 50,000 labeled images. Extensive experimental results and

*Both authors contributed equally to this research.

[†]Work done during the internship at Alibaba Group.

[‡]Corresponding author.

online A/B tests demonstrate that PAID can produce more visually appealing advertising images.

1 Introduction

Advertising images (as shown in Figure 1) are essential for commercial recommendation. Visually appealing and attractive images usually have high click-through rates [37] but are labor-intensive and time-consuming to create [34]. With the rapid advancement of generative methods [13, 24, 28, 33], it is now possible to automatically generate advertising images using only basic product inputs: a product foreground image, marketing taglines, and a target size.

Currently, generating advertising images using only the basic inputs mentioned above has rarely been explored. Existing methods [9, 20, 36, 39, 42] mainly focus on parts of the problem, such as background or layout generation, rather than offering a complete solution for integrating product foregrounds and taglines. Although these methods can be combined, they struggle to effectively highlight product images and taglines while maintaining visual appeal and harmony. Specifically, building on existing approaches [9, 20, 36, 39, 42], we can first utilize predefined rules to create background prompts. These prompts are then fed into text-to-image inpainting models to complete backgrounds for product foregrounds. Layouts for taglines and decorative elements (collectively referred to as graphic elements) are predicted based on the images and taglines. Finally, attribute prediction and graphics rendering techniques are employed to add these graphic elements to the images. However, this process has several limitations: a) Lack of adaptability: It cannot generate background prompts that match the specific content and shape of the product, leading to poor foreground-background harmony. b) Fixed foreground positioning: The position of the foreground cannot be adjusted based on its characteristics and the background prompt, potentially resulting in inappropriate product size and poor composition. c) Restricted tagline placement: When adding taglines, the whole image content is already set, limiting the available space for tagline placement.

In this paper, we propose a novel framework called Product-Centric Advertising Image Design (PAID) to enhance advertising image generation using only basic product inputs. While PAID remains a multistage process, we have refined its stages and task definitions to enhance foreground-background compatibility and the spatial arrangement of product foregrounds and taglines.

As illustrated in Figure 2, we first introduce a task to generate prompts, using a Visual Language Model (VLM) [8] to adaptively create background prompts that better match the scene, placement, and angle based on product foregrounds. Following this, we propose a layout generation task that arranges the graphic elements (marketing taglines and decorative underlays), product foreground, and other nongraphic elements (objects to be generated from the background prompt). This arrangement is based on the product foreground, background prompt, marketing taglines, and target size. By arranging the product foreground and marketing information concurrently, as opposed to generating the overall image first and then deciding the graphic layout, it becomes less constrained by the image content and allows for a more rational presentation of the product info. Furthermore, considering the nongraphic elements together helps minimize conflicts with taglines that could

affect readability and attractiveness. Next, we train an inpainting text-to-image model based on SDXL [26] that can be controlled by input layouts. Combining inpainting, layout, and prompt control effectively is challenging due to potential conflicts among multiple control signals. A LoRA [15] adaption strategy is adopted to balance conflicts and facilitate training. Since layout mainly influences higher-level abstract information, we apply layout control only in the deeper blocks of the UNet [11], combined with a multi-scale training strategy to enhance training stability and efficiency. Finally, we utilize an attribute prediction and graphics rendering module to overlay graphic elements onto the image. To build the framework and verify its effectiveness, we have collected and labeled over 50,000 images to establish datasets. In testing, PAID demonstrates its ability to produce advertising images with better visual quality. It has been deployed on two advertising recommendation scenarios of Taobao, and online A/B tests show that its generated images are more appealing to users.

In summary, our main contributions are as follows:

- We propose a novel framework PAID for advertising image design given only a product foreground image, taglines, and a target size. It centers on the product foreground and taglines to enhance the overall product prominence and improve the image aesthetics.
- A VLM is introduced to generate suitable prompts for image generation using the input product foreground image, considering product placement angle and shape.
- To arrange product foregrounds and taglines more effectively, a VLM-based layout generator is proposed. It can mix and arrange graphic and nongraphic elements with the target size and prompt. Accordingly, an image generation model that simultaneously accepts layout, prompt, and foreground control is proposed. Several strategies are introduced to enhance effectiveness and efficiency.
- We have collected and labeled over 50,000 images to create datasets for advertising image generation. The effectiveness of our method has been validated through tests on this dataset and online A/B tests in real advertising scenarios.

2 Related Work

2.1 Advertising Image Design

In recent years, many methods have been proposed to automate advertising image design [14, 17, 19, 20, 30, 42]. They can be divided into two subcategories: background-based and foreground-based methods. Background-based methods predict graphic layouts based on complete images (not only product foregrounds), followed by attribute prediction and graphics rendering modules to create the final advertising image. CGL-GAN [42] and DS-GAN [14] design transformer architectures to leverage image info and generate layouts. RADM [17] is the first to simultaneously consider the image and tagline content to derive layouts with a diffusion model. PosterLlama [30] leverages the rich design knowledge in Large Language Models (LLMs) to predict the layout. AutoPoster [20] introduces a complete pipeline which first generates a layout based on a complete image, and then predicts the attributes of graphic elements

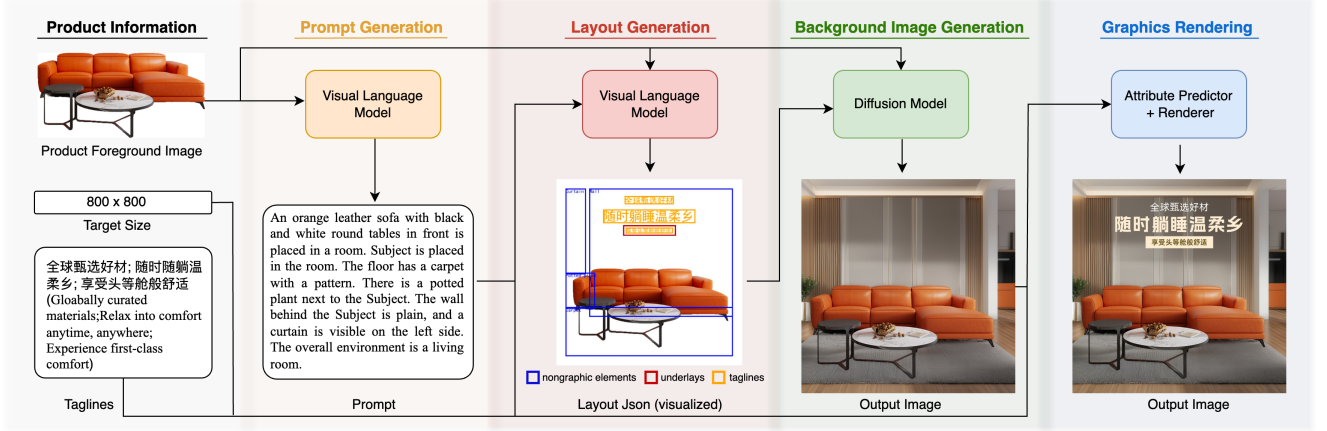


Figure 2: Pipeline of PAID. It consists of four stages and generates advertising images centered around product information.

and renders them onto the image. For these methods, the spatial layout is restricted due to fixed image content, which further restricts the tagline content, including the number and length of taglines.

In contrast, P&R [19] is a foreground-based method that leverages both the product foreground image and tagline content to predict the layout of the product foreground and taglines. It subsequently designs a module network to outpaint the background and render the taglines according to the given background prompt and generated layout. The tagline content is not limited, and the layout is more flexible. However, P&R ignores the harmony between the background prompt and the generated layout. The layout may conflict with background generation. In our PAID framework, the overall layout of graphic elements, product foreground, and other nongraphic elements is generated jointly according to the product foreground, background prompt, and tagline contents, aiming to achieve the best harmony among them.

2.2 Controllable Image Generation

There have been significant developments in text-to-image models [26, 28]. To control instances and further improve image quality, some methods introduce layout guidance, dividing into training-free and training-based categories. Training-free methods manipulate the attention map [16] or compute attention-based loss during de-noising [1, 5, 6, 40]. Training-based methods, like GLIGEN [18] and InstanceDiffusion [38], modify network architecture, incorporating layout data by adding gated self-attention layers.

For advertising image generation [3, 9, 19, 35], text-to-image models equipped with inpainting capabilities are frequently utilized. The inpainting technique is employed to preserve product characteristics, while the prompt is used to describe the background. The foreground image is utilized by incorporating extra channels into the UNet architecture [28] or employing an inpainting ControlNet [41]. To better control the overall layout of advertising images and improve the quality of generated images, we combine inpainting with layout control. Currently, there is limited exploration in this area. SceneBooth [4] is the first model to integrate both controls in training, combining gated self-attention layers and inpainting ControlNet to train a model based on SD 1.5 [28] that can accept

layout and foreground controls. However, directly combining the two to train a larger model like SDXL can lead to non-convergence or a decline in the quality of generated images. Therefore, we use several strategies when training the layout-controlled inpainting model to ensure training stability, generation quality, and efficiency.

3 PITA Dataset and PIL Dataset

For automatic image design of product-centric advertising, we collect a large-scale Product-Centric Image-Tagline Advertising (PITA) dataset, gathering 38,017 samples from e-commerce platforms and the CGL dataset [42]. 1,000 of them are used for testing. PITA is a dataset of varying sizes, featuring images with four distinct aspect ratios: 0.684, 1.0, 0.667, and 0.75. Each image is labeled with prompts (foreground caption and background caption), a product mask, and a layout of graphic and nongraphic elements. Each element is represented with a type and a bounding box (bbox). The graphic elements contain “Logo”, “Tagline”, and “underlay”. Some examples of data visualization are in the appendix.

For layout-controlled background inpainting, we additionally construct a Product-Centric Image Layout (PIL) dataset. The images do not contain graphic elements and are labeled with prompts, product masks, and layouts of nongraphic elements. PIL contains 12,247 samples in total and 1,000 of them are divided for test.

4 Method

4.1 Overall Framework

As illustrated in Figure 2, our proposed PAID framework consists of four stages: prompt generation, layout generation, background image generation, and graphics rendering.

4.2 Prompt generation

For prompt generation, we fine-tune a large vision-language model π_{prompt} based on InternLM-XComposer2-v1 (XCP2) [8]. The method is illustrated in the upper part of Figure 3.

Input data format. For the input of LLM, we first describe the prompt generation task and ask for foreground and background descriptions. For the image input, we crop out the product foreground and feed it into the visual encoder.

Output data format. To enable downstream layout and background image generation tasks, and to better understand the relationship between the foreground and background, we use the prompt generation model π to simultaneously predict the foreground description p_{fore} and the background prediction p_{back} . We format the output in JSON as it is compatible with the pre-trained VLM and simplifies the following analysis. The output JSON is structured as $p = (p_{fore}, p_{back})$.

Training scheme. A standard VLM training scheme involves two stages: pre-training and supervised fine-tuning (SFT) [21]. During pre-training, the projector learns to align features between visual and text modalities. In the SFT stage, the projector and LLM are further trained for visual understanding tasks. Since we utilize the VLM trained after the SFT stage, the model can understand input images and follow instructions. We only fine-tune the LLM branch with our dataset to adapt the model to the prompt generation task, using cross-entropy loss as the objective function. The model π_{prompt} takes the foreground image I_{fore} and predefined instructions as input, performing two main tasks: generating a foreground description p_{fore} and predicting the background description p_{back} . The prompt generation process is as follows:

$$p = \pi_{prompt}(I_{fore}). \quad (1)$$

4.3 Layout generation

In this stage, we introduce the Jointly Predict Graphic and Non-graphic Layout (JPGNL) method, which optimizes the arrangement and improves the tagline readability and image appeal. It predicts the layout of graphic elements, the product, and other nongraphic elements based on the foreground image, prompt, taglines, and target size. Similar to prompt generation, we use XCP2 [8] for layout generation. The method is shown in the lower part of Figure 3.

Input data format. For the input to the LLM, we describe the layout generation task and organize input conditions in JSON format. The image input remains the same as in prompt generation. A target canvas aspect ratio is given as a condition to support multi-scale layout design. The aspect ratio of the product foreground is provided to help keep its shape. Foreground and background prompts are also given for generating the image layout. For the pre-defined taglines, we list them with empty locations and expect the model to complete them. If a logo is needed, we include it as a condition in the graphic layout section and specify its aspect ratio.

Except for these basic conditions, we also take product characteristics into account. In E-commerce scenarios, some products should not be occluded for better display. While for others, like clothing or human-hold items, partial occlusion is acceptable. To differentiate between these, we introduce a Class-Conditioned Layout Prediction (CCLP) strategy. CCLP provides clear information about the product class and whether foreground occlusion is allowed. For the not-allowing occlusion set (No Occ Set), we describe ‘‘The class of subject is [V1]. The bounding boxes of taglines should never occlude the subject’’. For the allowing occlusion set (Allow Occ Set),

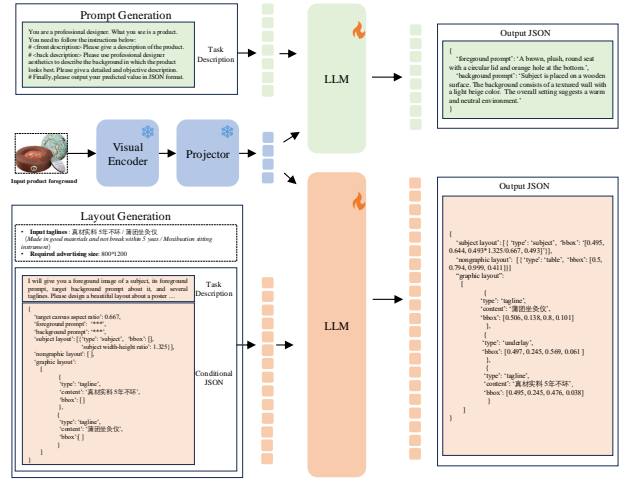


Figure 3: The framework of our prompt and layout generation model and data format.

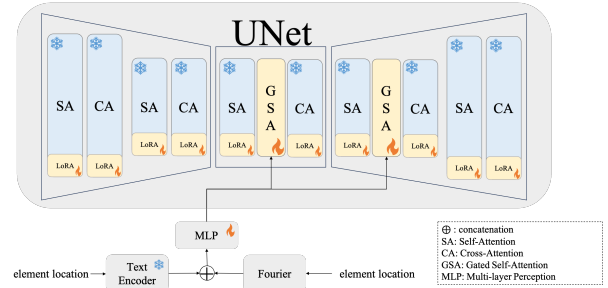


Figure 4: Layout control in the image generation model.

the description is ‘‘The class of subject is [V2]. The bounding boxes of taglines are allowed to occlude the subject’’.

Output data format. The output layout is structured in JSON format with three parts: subject layout, other nongraphic layout, and graphic layout. To maintain the shape of the product foreground, we propose a Ratio-Keeping Bbox Representation (RKBR). It is expressed as $[x, y, h \cdot r1/r2, h]$. (x, y) is the normalized center point. w and h are the normalized width and height. $r1$ and $r2$ are the actual aspect ratio of the foreground and canvas, respectively. Each value ranges from 0 to 1 with three decimal places. The nongraphic layout contains the location of elements in the background prompt, each having a type (instance name) and bounding box (bbox). The graphic layout defines each element by type, content, and bounding box, covering tagline, underlay, and logo. The content key is used only for tagline types to specify its semantic content. Bounding boxes are listed as $[x, y, w, h]$. The model is expected to supplement underlay adaptively. If logos are required, it is represented in the same way as the product for ratio keeping.

Training scheme. Same as the prompt generation module, we only fine-tune the LLM branch with the visual encoder and projector frozen. The output JSON is structured to predict the layout in a raster scan order, adhering to the ascending order of top-left

coordinates. Furthermore, we shuffle the taglines in the input conditional JSON for data augmentation and prevent the model from memorizing the input sequence.

4.4 Background Image generation

In this process, we train an SDXL-based [26] image generation model controlled by product foreground, prompt, and layout.

Layout control. Suppose that there are N elements to be drawn in an image, represented as $\{(n_i, l_i) | i = 0, 1, \dots, N-1\}$. We map these into N embeddings as layout input. Here, n_i is the element name, and l_i is its location. Concretely, we use the text encoder in SDXL to map n_i into a global semantic embedding $\mathbf{e}_{n,i}$. l_i is transferred into normalized top-left and bottom-right coordinates, then fed into a Fourier mapping layer[32], deriving the location embedding $\mathbf{e}_{l,i}$. Next, $\mathbf{e}_{n,i}$ and $\mathbf{e}_{l,i}$ are concatenated and fed into a trainable MLP layer to represent the layout information of the i -th element, denoted as \mathbf{e}_i . $\mathbf{e} = \{\mathbf{e}_i | i = 0, 1, \dots, N-1\}$ is the layout embeddings. A gated self-attention (GSA) layer [18] is inserted between the self- and cross-attention layers in the original UNet to inject layout embeddings. Supposing there are M visual embeddings (\mathbf{V}) after the self-attention layer. The output of the GSA layer is

$$GSA(\mathbf{V}, \mathbf{E}) = \mathbf{V} + \tanh(\gamma) * SA(cat(\mathbf{V}, \mathbf{E}))[:, M],$$

where γ is a learnable parameter, cat means concatenation, and SA means self-attention.

Considering that the layout is semantic-level information and less related to high-frequency details, we only add GSA layers in the deep blocks of UNet. We refer to this strategy as Deep Layer Control (DLC). Specifically, the layout control is applied in the middle block and the lowest resolution of up blocks. This reduces the parameters and inference latency, and has no negative impact on generation quality. Additionally, we adopt a LoRA Adaptation Training (LAT) strategy in which trainable LoRA [15] layers are added to UNet, to bridge the gap between the base model and added GSA layers. This further accelerates convergence and increases generation quality. Figure 4 describes how layout control is achieved.

Training stages. To build the product reservation layout-to-image model, training involves two steps. First, we modify the UNet architecture in SDXL by adding the above GSA layers and train it to derive a layout-to-image model. We use a multi-scale training strategy for faster convergence, first training on 512x512 resolution images and then fine-tuning on 1024x1024 resolution images. Second, we equip the trained model with an inpainting ControlNet and further fine-tune it on 1024x1024 resolution images. This step incorporates the product foreground, achieving full control over the prompt, layout, and product foreground.

4.5 Graphics Rendering

Since there is no effective method to predict the visual attributes of graphic elements, and the graphics rendering module is not the focus of this paper, we design a strategy according to the aesthetic rules to handle graphics rendering. We first sort the tagline elements by area to decide the font and color, both of which are limited to a specific set [23]. The selection is based on the similarity to the foreground color and contrast with the background area. Taglines grouped by size and position use the same font and color. For the underlay, the color is chosen based on its contrast with the tagline

color and similarity to the background color. The shape is selected from a predefined Scalable Vector Graphics (SVG) library based on its size and proportions, with minor adjustments for fitting.

5 Experiments

In this section, we compare our PAID framework and its modules with previous ones. We conducted experiments on the PITA dataset, and the results confirm the effectiveness of our method.

5.1 Implementation Details

For prompt and layout generation, XCP2 [8] is used as our backbone. Its visual encoder is built upon CLIP ViT-Large [27], processing 490x490 resolution images. The LLM is based on InternLM2 [2]. We fine-tune the LLM branch on the PITA dataset for one epoch. We train the model using AdamW optimizer with a learning rate of $1e-5$. Batch size on each GPU is set to 1, and gradient accumulation of 8 is adopted. The training costs about 14 hours with 8 NVIDIA A100 GPUs. During inference, we use top-p sampling with p set to 0.9 and a sampling temperature of 0.6.

For background image generation, we use the SDXL base model as the backbone. During the first step, about 6.8 million high-aesthetic internal images with layout annotations are used. We train the newly added layers with a learning rate of $5e-5$ for 20k steps on 512x512 resolution and further fine-tune them with a learning rate of $2e-5$ for 20k steps on 1024x1024 resolution. Then in step 2, we introduce an inpainting ControlNet, which is pre-trained with millions of advertising images from E-commerce platforms [7], and fine-tune the layout-related layers with a learning rate of $2e-5$ for 1k steps, using 12k training data in the collected PIL dataset.

5.2 Evaluation Metrics

To evaluate the overall poster generation and each module, we use the following metrics.

Overall pipeline. We evaluate the overall pipeline from three perspectives: overall visual quality, and layout. For visual quality, we employ the Fréchet Inception Distance (FID) [12] and aesthetic score. The aesthetic score comes from advertising experts ranking the outputs of different methods. The average rank represents the mean aesthetic rating, with a lower rank indicating better creative results. For layout, we adopt the metrics used in previous studies [30, 42], which are detailed in the subsequent Layout Generation module.

Prompt generation. We evaluate prompt generation quality based on fore-background matching rate (FBM rate) and e-commerce domain score (ED score). FBM Rate refers to how well a product foreground fits with a given prompt background. We classify this matching into “reasonable” or “unreasonable” through human annotation, and calculate the proportion of reasonable cases. ED Score assesses how well the model-generated prompts reflect e-commerce characteristics. We calculate the FID between the CLIP features of these prompts and the ground truth prompts in the test set.

Layout generation. Following previous work [30, 42], we use graphic metrics and content metrics to evaluate layouts. Graphic metrics focus on relationships between graphic elements, including validity Val , alignment Ali , overlap Ove , and underlay Und_s . Val means the ratio of elements larger than 0.1% of the canvas. Ali



Figure 5: Visualization of advertising images designed by different methods.

assesses how well elements are spatially aligned. Ove is the average intersection over union (IoU) of all element pairs except for underlays. Und_l and Und_s checks if underlays enhance non-underlay elements. Content metrics assess the harmony of layout with the image, including utility Uti , occlusion Occ , and unreadability Rea . Uti evaluates space usage for graphic elements. Occ is the average overlapping area between the graphic elements and products. Rea represents the non-flatness of regions that tagline elements without underlays are put on. For methods that take taglines as input, we report the tagline match rate (TMR), to see if the number of generated tagline bboxes is consistent with input taglines.

Background image generation. We evaluate the quality of generated images with FID, CLIP-T [29], CLIP-I [10]. To verify layout control, we use Grounding-DINO [22] to detect instances and calculate the maximum IoU between detected bboxes and ground-truth bboxes. The average of these maximum IoUs is called mIOU. In addition, Grounding-DINO AP scores are also reported.

5.3 Comparison

Compare with automatic pipelines for advertising image design. Since there are no public methods for advertising image design conditioned on the product foreground, taglines, and target size, we design two pipelines for comparison. **Pipeline 1** use GPT-4o [25] for prompt and layout generation. We also finetune the SDXL-based inpainting model on our PIL dataset. The only difference between this method and ours is the absence of layout control and the corresponding training stage. During inference, only the

product foreground is controlled by the layout output of GPT-4o. **Pipeline 2** first generate a background prompt using GPT-4o. The image generation model is the same as in Pipeline 1, but during inference, the foreground is placed according to general aesthetic rules. Next, the image and taglines are processed by the SOTA layout generation model PosterLlama to generate a graphic layout. Last, the results of these two pipelines are processed through the same graphics rendering module as our method to produce the final image. Table 1 shows the quantitative comparison. PAID outperforms in most metrics, except for slightly higher occlusion compared to Pipeline 1, which places the product centrally with a small bounding box. However, Pipeline 1 uses GPT-4o for layout, lacking product-centric design knowledge, resulting in lower quality. PAID uses trained experts for different tasks in ad design, creating more visually appealing results (see Figure 5). Pipeline 2 fixes the product location, limiting adaptability to product shapes, whereas PAID adjusts layouts based on product shape for better visuals. Additionally, the fixed background of Pipeline 2 can lead to layouts with crowded tagline boxes, making them hard to read, while our model provides more flexible and readable layouts.

Table 1: Quantitative comparison between automatic pipelines for product-centric advertising image design.

Method	Overall Visual Quality		Layout Quality						
	Fid↓	Aesthetic↓	Ove↓	Ali↓	Und _l ↑	Und _s ↑	Uti↑	Occ↓	Rea↓
Pipeline 1	56.545	2.781	0.0021	0.002	0.8333	0.7872	0.0891	0.0937	0.234
Pipeline 2	43.221	1.814	0.0016	0.0028	0.9994	0.9930	0.0984	0.1158	0.1864
PAID	37.524	1.405	0.0013	0.0017	0.9999	0.9973	0.1367	0.0955	0.1815

Compare with prompt generation methods. For prompt comparison, we use GPT-4o and an untrained version of our model (XCP2) as baselines. Both utilize in-context learning (ICL) for optimal performance. The FBM Rate is determined by votes from three annotators for each case. As shown in Table 2, our method outperforms the baselines in both FBM Rate and ED Score. This means that our model effectively aligns with the e-commerce prompt dataset distribution after training. We also visualize the feature distribution of prompts generated in the appendix.

Table 2: Evaluation of prompt generation methods.

Method	FBM Rate \uparrow	ED Score \downarrow
GPT-4o	97.9%	22.49
XCP2	94.8%	13.04
Finetuned XCP2	98.5%	7.17

Compare with layout generation methods. To verify the advantage of our layout generation model, we compare it with previous background-based methods (DS-GAN [14], RADM [17], and PosterLlama [30]) and the foreground-based method P&R [19]. For background-based generation methods, we conduct experiments on two versions of the testing set for fair comparison, named the erased/generated set. The erased set contains images with graphic elements erased by LaMa [31], which may provide hints to put graphic elements on these erased areas. The generated set contains images re-generated using their ground-truth prompts (image captions). The generated set has no above hints and conforms to real applications. As for the foreground-based method P&R, since it has not released the codes, we re-implement its core idea: first, generating the layout of the foreground and graphic elements conditioned on the foreground and taglines, and second, generating the final image based on the background prompt, layout, and foreground. Our method uses the ground-truth prompt, product foreground, and taglines for prediction. The results are shown in Table 3 and Figure 6. Background-based methods perform relatively poorly in terms of product occlusion and overlap and alignment of graphic elements. This may be due to the fixed background image content, leaving less room for the model flexibility. RADM and DS-GAN, which are insensitive to tagline content, also face issues with generating tagline boxes that cannot adequately fill the tagline content. The foreground-based method P&R improves in these areas but does not consider the harmony between the product, background prompt, and graphic layout, sometimes leading to unreasonable generated images. Our method, PAID, takes into account the shape of the product foreground, background prompt, and tagline content to decide the overall layout, including graphic and nongraphic elements, resulting in a better overall effect.

Compare with layout-controlled inpainting models. We compare our layout-controlled background image generation model with others, including training-based method GLIGEN [18] and training-free methods BoxDiff [40], TFCLG [6], and MultiDiffusion [1]. Since these methods lack inpainting ability, we re-implement them with the SDXL-based inpainting ControlNet [7]. Quantitative results are reported in Table 4. Training-free methods have weaker spatial control compared to training-based methods. Our trained

Table 3: Quantitative performance comparison of layout generation methods. The bold number represents the best result in each column except for the erased set. BG/FG-based are the abbreviations for Background/Foreground-based methods.

	Method	Val \uparrow	Ove \downarrow	Ali \downarrow	Und \downarrow	Und \downarrow	Uti \uparrow	Occ \downarrow	Rea \downarrow	TMR \uparrow
BG-based (Erased)	DS-GAN[14]	0.9585	0.0270	0.0058	0.3910	0.0744	0.1816	0.1063	0.1826	-
	RADM[17]	0.999	0.0411	0.0017	0.9852	0.6934	0.1484	0.0814	0.1722	0.82
	PosterLlama[30]	0.9984	0.002	0.0026	0.9899	0.9870	0.1226	0.0976	0.1820	0.998
BG-based (Generated)	DS-GAN[14]	0.9621	0.0284	0.0080	0.3350	0.0528	0.1701	0.1202	0.2328	-
	RADM[17]	0.9753	0.0484	0.0201	0.7997	0.2828	0.0657	0.2527	0.2558	0.289
	PosterLlama[30]	1.0	0.0015	0.0022	0.9990	0.9965	0.1090	0.1208	0.231	0.996
	P&R*[19]	1.0	0.0012	0.0019	0.9966	0.9929	0.1367	0.1000	0.2008	1.0
FG-based	Ours	1.0	0.0012	0.0017	0.9976	0.9956	0.1364	0.0973	0.1968	1.0

model outperforms others in FID, mIoU, and AP, indicating better image quality and spatial control. As shown in Figure 7, other models tend to miss some instances when more objects are required, while our model generates them more accurately.

Table 4: Quantitative performance comparison of layout-controlled inpainting models on PIL test set.

Method	FID \downarrow	CLIP-T \uparrow	CLIP-I \uparrow	mIoU \uparrow	AP/AP50/AP75 \uparrow
BoxDiff[40]	29.383	0.315	0.896	0.555	0.037/0.064/0.033
TFCLG[6]	29.498	0.315	0.895	0.543	0.033/0.056/0.029
MultiDiffusion[1]	42.359	0.311	0.841	0.5617	0.029/0.052/0.025
GLIGEN[18]	27.237	0.312	0.898	0.561	0.047/0.073/0.044
Ours	25.917	0.313	0.906	0.705	0.079/0.127/0.078

5.4 Online Result

To assess the online performance of PAID, we conduct A/B tests in two advertising recommendation scenarios on Taobao. We randomly select 5,000 products from various categories (including clothing, cosmetics, food, and electronics) and collect their foreground images and taglines from the advertisers. We then generate advertising images for each product using both PAID and Pipeline 2 (the top-performing baseline as shown in Table 1). The A/B tests are conducted using 5% of the main traffic, affecting only the experimental products when this traffic is directed to them. After gathering data over one month, we found that PAID achieved a 3.02% and 3.03% increase in click-through rate (CTR) for the two recommendation scenarios, respectively. This indicates that PAID is capable of producing more visually appealing advertising images, resulting in improved recommendation outcomes.

6 Conclusion

In this paper, a novel framework named Product-Centric Advertising Image Design (PAID) is proposed to automatically create advertising images only based on product foreground images, marketing taglines, and target sizes. PAID consists of four stages: prompt generation, layout generation, background image generation, and graphics rendering. First, it generates adaptive prompts according to the product foregrounds. Then, it predicts how graphic and nongraphic elements should be placed according to the prompt, product foreground, and taglines, creating a harmonious overall layout. Next, a layout-controlled inpainting model is utilized for background image generation. A graphics rendering module is then applied to get the final images. We train separate experts to conduct

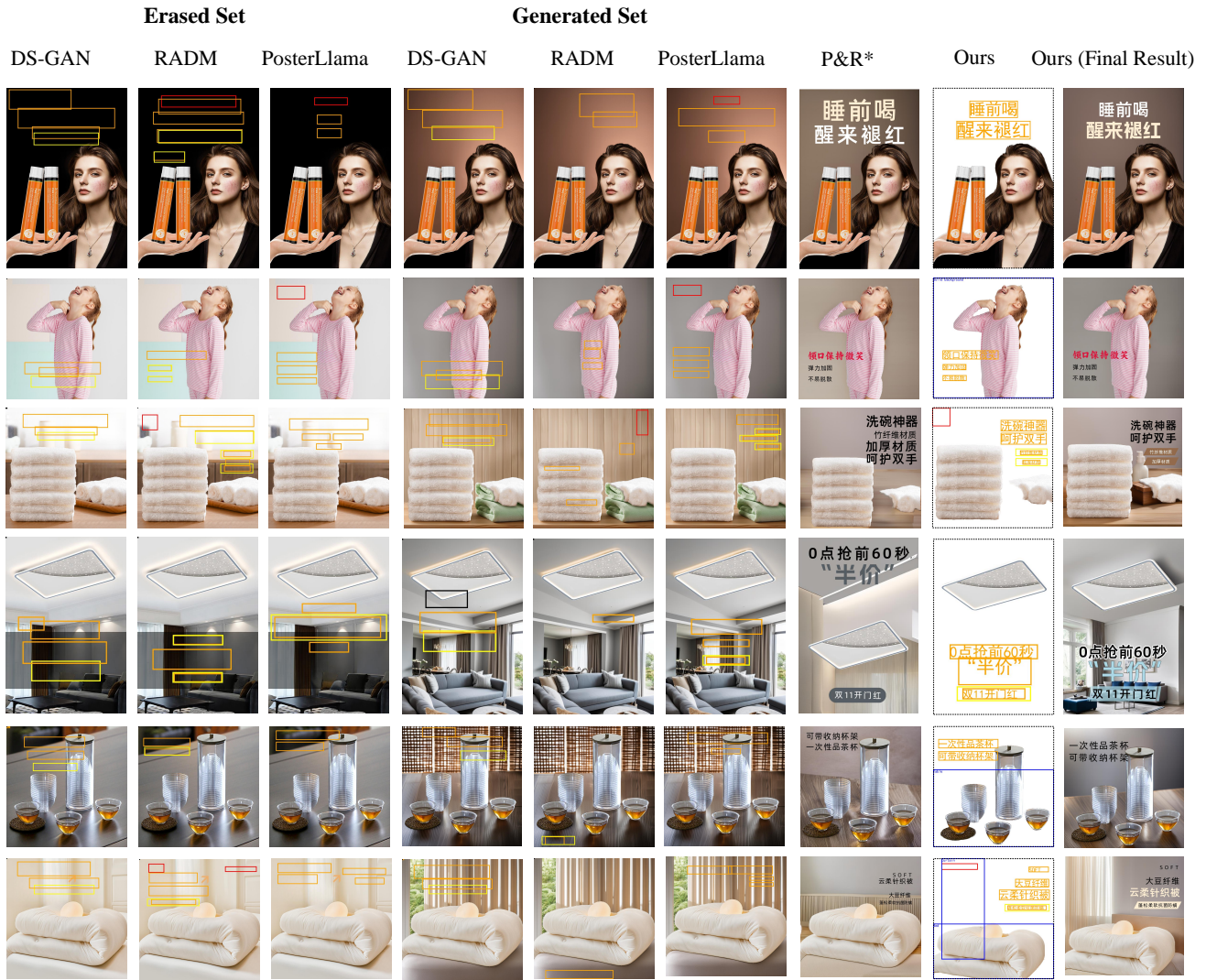


Figure 6: Qualitative comparison of layout generation methods. Orange: tagline, Yellow: underlay, Red: logo, Black: Invalid.



Figure 7: Visualization of images generated by different layout-controlled inpainting models.

these sub-tasks. Two datasets are created for the convenience of training and testing. The results of the test set and the online A/B

tests have proven that the proposed PAID framework generates more visually pleasing and attractive advertising images.

Acknowledgements

This work is supported by National Natural Science Foundation of China (NSFC No.62076031 and No.62076036) and Alibaba Research Intern Program.

References

- [1] Omer Bar-Tal, Lior Yariv, Yaron Lipman, and Tali Dekel. 2023. Multidiffusion: Fusing diffusion paths for controlled image generation. (2023).
- [2] Zheng Cai, Maosong Cao, Haojong Chen, Kai Chen, Keyu Chen, Xin Chen, Xun Chen, Zehui Chen, Zhi Chen, Pei Chu, et al. 2024. Internlm2 technical report. *arXiv preprint arXiv:2403.17297* (2024).
- [3] Tingfeng Cao, Junsheng Kong, Xue Zhao, Wenqing Yao, Junwei Ding, Jinhui Zhu, and Jiandong Zhang. 2024. Product2IMG: Prompt-Free E-commerce Product Background Generation with Diffusion Model and Self-Improved LMM. In *Proceedings of the 32nd ACM International Conference on Multimedia*. 10774–10783.
- [4] Shang Chai, Zihang Lin, Min Zhou, Xubin Li, Liansheng Zhuang, and Houqiang Li. 2025. SceneBooth: Diffusion-based Framework for Subject-preserved Text-to-Image Generation. *arXiv preprint arXiv:2501.03490* (2025).
- [5] Hila Chefer, Yuval Alaluf, Yael Vinker, Lior Wolf, and Daniel Cohen-Or. 2023. Attend-and-excite: Attention-based semantic guidance for text-to-image diffusion models. *ACM Transactions on Graphics (TOG)* 42, 4 (2023), 1–10.
- [6] Minghao Chen, Iro Laina, and Andrea Vedaldi. 2024. Training-free layout control with cross-attention guidance. In *Proceedings of the IEEE/CVF Winter Conference on Applications of Computer Vision*. 5343–5353.
- [7] Alimama Creative. 2024. https://huggingface.co/alimama-creative/EcomXL_controlnet_inpaint.
- [8] Xiaoyi Dong, Pan Zhang, Yuhang Zang, Yuhang Cao, Bin Wang, Linke Ouyang, Xilin Wei, Songyang Zhang, Haodong Duan, Maosong Cao, et al. 2024. Internlm-xcomposer2: Mastering free-form text-image composition and comprehension in vision-language large model. *arXiv preprint arXiv:2401.16420* (2024).
- [9] Zhenbang Du, Wei Feng, Haohan Wang, Yaoyu Li, Jingsen Wang, Jian Li, Zheng Zhang, Jingjing Lv, Xin Zhu, Junsheng Jin, et al. 2024. Towards Reliable Advertising Image Generation Using Human Feedback. In *European Conference on Computer Vision*. Springer, 399–415.
- [10] Rinon Gal, Yuval Alaluf, Yuval Atzmon, Or Patashnik, Amit H Bermano, Gal Chechik, and Daniel Cohen-Or. 2022. An image is worth one word: Personalizing text-to-image generation using textual inversion. *arXiv preprint arXiv:2208.01618* (2022).
- [11] Kaiming He, Xiangyu Zhang, Shaoqing Ren, and Jian Sun. 2016. Deep Residual Learning for Image Recognition. In *2016 IEEE Conference on Computer Vision and Pattern Recognition, CVPR 2016, Las Vegas, NV, USA, June 27-30, 2016*. IEEE Computer Society, 770–778. <https://doi.org/10.1109/CVPR.2016.90>
- [12] Martin Heusel, Hubert Ramsauer, Thomas Unterthiner, Bernhard Nessler, and Sepp Hochreiter. 2017. Gans trained by a two time-scale update rule converge to a local nash equilibrium. *Advances in neural information processing systems* 30 (2017).
- [13] Jonathan Ho, Ajay Jain, and Pieter Abbeel. 2020. Denoising diffusion probabilistic models. *Advances in neural information processing systems* 33 (2020), 6840–6851.
- [14] Hsiao Yuan Hsu, Xiangteng He, Yuxin Peng, Hao Kong, and Qing Zhang. 2023. Posterlayout: A new benchmark and approach for content-aware visual-textual presentation layout. In *Proceedings of the IEEE/CVF Conference on Computer Vision and Pattern Recognition*. 6018–6026.
- [15] Edward J Hu, Yelong Shen, Phillip Wallis, Zeyuan Allen-Zhu, Yuanzhi Li, Shean Wang, Lu Wang, and Weizhu Chen. 2021. Lora: Low-rank adaptation of large language models. *arXiv preprint arXiv:2106.09685* (2021).
- [16] Yunji Kim, Jiyoung Lee, Jin-Hwa Kim, Jung-Woo Ha, and Jun-Yan Zhu. 2023. Dense text-to-image generation with attention modulation. In *Proceedings of the IEEE/CVF International Conference on Computer Vision*. 7701–7711.
- [17] Fengheng Li, An Liu, Wei Feng, Honghe Zhu, Yaoyu Li, Zheng Zhang, Jingjing Lv, Xin Zhu, Junjie Shen, Zhangang Lin, et al. 2023. Relation-aware diffusion model for controllable poster layout generation. In *Proceedings of the 32nd ACM International Conference on Information and Knowledge Management*. 1249–1258.
- [18] Yuheng Li, Haotian Liu, Qingyang Wu, Fangzhou Mu, Jianwei Yang, Jianfeng Gao, Chunyuan Li, and Yong Jae Lee. 2023. Gligen: Open-set grounded text-to-image generation. In *Proceedings of the IEEE/CVF Conference on Computer Vision and Pattern Recognition*. 22511–22521.
- [19] Zhaochen Li, Fengheng Li, Wei Feng, Honghe Zhu, An Liu, Yaoyu Li, Zheng Zhang, Jingjing Lv, Xin Zhu, Junjie Shen, et al. 2023. Planning and Rendering: Towards End-to-End Product Poster Generation. *arXiv preprint arXiv:2312.08822* (2023).
- [20] Jinpeng Lin, Min Zhou, Ye Ma, Yifan Gao, Chenxi Fei, Yangjian Chen, Zhang Yu, and Tiezheng Ge. 2023. Autoposter: A highly automatic and content-aware design system for advertising poster generation. In *Proceedings of the 31st ACM International Conference on Multimedia*. 1250–1260.
- [21] Haotian Liu, Chunyuan Li, Qingyang Wu, and Yong Jae Lee. 2024. Visual instruction tuning. *Advances in neural information processing systems* 36 (2024).
- [22] Shilong Liu, Zhaoyang Zeng, Tianhe Ren, Feng Li, Hao Zhang, Jie Yang, Qing Jiang, Chunyuan Li, Jianwei Yang, Hang Su, et al. 2024. Grounding dino: Marrying dino with grounded pre-training for open-set object detection. In *European Conference on Computer Vision*. Springer, 38–55.
- [23] Zeyu Liu, Weicong Liang, Zhanhao Liang, Chong Luo, Ji Li, Gao Huang, and Yuhui Yuan. 2024. Glyph-byt5: A customized text encoder for accurate visual text rendering. In *European Conference on Computer Vision*. Springer, 361–377.
- [24] Jacob Menick and Nal Kalchbrenner. 2018. Generating latent diffusion models with subscale pixel networks and multidimensional upscaling. *arXiv preprint arXiv:1812.01608* (2018).
- [25] OpenAI. 2024. <https://openai.com/index/hello-gpt-4o/>.
- [26] Dustin Podell, Zion English, Kyle Lacey, Andreas Blattmann, Tim Dockhorn, Jonas Müller, Joe Penna, and Robin Rombach. 2023. Sdxl: Improving latent diffusion models for high-resolution image synthesis. *arXiv preprint arXiv:2307.01952* (2023).
- [27] Alec Radford, Jong Wook Kim, Chris Hallacy, Aditya Ramesh, Gabriel Goh, Sandhini Agarwal, Girish Sastry, Amanda Askell, Pamela Mishkin, Jack Clark, et al. 2021. Learning transferable visual models from natural language supervision. In *International conference on machine learning*. PMLR, 8748–8763.
- [28] Robin Rombach, A. Blattmann, Dominik Lorenz, Patrick Esser, and Björn Ommer. 2021. High-Resolution Image Synthesis with Latent Diffusion Models. *2022 IEEE/CVF Conference on Computer Vision and Pattern Recognition (CVPR)* (2021), 10674–10685. <https://api.semanticscholar.org/CorpusID:245335280>
- [29] Nataniel Ruiz, Yuanzhen Li, Varun Jampani, Yael Pritch, Michael Rubinstein, and Kfir Aberman. 2023. Dreambooth: Fine tuning text-to-image diffusion models for subject-driven generation. In *Proceedings of the IEEE/CVF conference on computer vision and pattern recognition*. 22500–22510.
- [30] Jaeyung Seol, Seojun Kim, and Jaeyun Yoo. 2024. PosterLlama: Bridging Design Ability of Language Model to Contents-Aware Layout Generation. *arXiv preprint arXiv:2404.00995* (2024).
- [31] Roman Suvorov, Elizaveta Logacheva, Anton Mashikhin, Anastasia Remizova, Arsenii Ashukha, Aleksei Silvestrov, Naejin Kong, Harshith Goka, Kiwoong Park, and Victor Lempitsky. 2022. Resolution-robust large mask inpainting with fourier convolutions. In *Proceedings of the IEEE/CVF winter conference on applications of computer vision*. 2149–2159.
- [32] Matthew Tancik, Pratul Srinivasan, Ben Mildenhall, Sara Fridovich-Keil, Nithin Raghavan, Utkarsh Singhal, Ravi Ramamoorthi, Jonathan Barron, and Ren Ng. 2020. Fourier features let networks learn high frequency functions in low dimensional domains. *Advances in neural information processing systems* 33 (2020), 7537–7547.
- [33] Aaron Van Den Oord, Nal Kalchbrenner, and Koray Kavukcuoglu. 2016. Pixel recurrent neural networks. In *International conference on machine learning*. PMLR, 1747–1756.
- [34] Shanu Vashishtha, Abhinav Prakash, Lalitesh Morishetti, Kaushiki Nag, Yokila Arora, Sushant Kumar, and Kannan Achan. 2024. Chaining Text-to-Image and Large Language Model: A Novel Approach for Generating Personalized e-commerce Banners. In *Proceedings of the 30th ACM SIGKDD Conference on Knowledge Discovery and Data Mining, KDD 2024, Barcelona, Spain, August 25-29, 2024*, Ricardo Baeza-Yates and Francesco Bonchi (Eds.). ACM, 5825–5835. <https://doi.org/10.1145/3637528.3671636>
- [35] Haohan Wang, Wei Feng, Yang Lu, Yaoyu Li, Zheng Zhang, Jingjing Lv, Xin Zhu, Junjie Shen, Zhangang Lin, Lixing Bo, et al. 2023. Generate E-commerce Product Background by Integrating Category Commonality and Personalized Style. *arXiv preprint arXiv:2312.13309* (2023).
- [36] Shaodong Wang, Yunyang Ge, Liuhan Chen, Haiyang Zhou, Qian Wang, Xinhua Cheng, and Li Yuan. 2024. Prompt2Poster: Automatically Artistic Chinese Poster Creation from Prompt Only. In *ACM Multimedia 2024*.
- [37] Shiyao Wang, Qi Liu, Tiezheng Ge, Defu Lian, and Zhiqiang Zhang. 2021. A hybrid bandit model with visual priors for creative ranking in display advertising. In *Proceedings of the web conference 2021*. 2324–2334.
- [38] Xudong Wang, Trevor Darrell, Sai Saketh Rambhatla, Rohit Girdhar, and Ishan Misra. 2024. Instancediffusion: Instance-level control for image generation. In *Proceedings of the IEEE/CVF Conference on Computer Vision and Pattern Recognition*. 6232–6242.
- [39] Haohan Weng, Danqing Huang, Yu Qiao, Zheng Hu, Chin-Yew Lin, Tong Zhang, and CL Chen. 2024. Design: A Pipeline for Controllable Design Template Generation. In *Proceedings of the IEEE/CVF Conference on Computer Vision and Pattern Recognition*. 12721–12732.
- [40] Jinheng Xie, Yuexiang Li, Yawen Huang, Haozhe Liu, Wentian Zhang, Yefeng Zheng, and Mike Zheng Shou. 2023. Boxdiff: Text-to-image synthesis with training-free box-constrained diffusion. In *Proceedings of the IEEE/CVF International Conference on Computer Vision*. 7452–7461.
- [41] Lvmin Zhang, Anyi Rao, and Maneesh Agrawala. 2023. Adding conditional control to text-to-image diffusion models. In *Proceedings of the IEEE/CVF International Conference on Computer Vision*. 3836–3847.

- [42] Min Zhou, Chenchen Xu, Ye Ma, Tiezheng Ge, Yuning Jiang, and Weiwei Xu. 2022. Composition-aware Graphic Layout GAN for Visual-Textual Presentation Designs. In *Proceedings of the Thirty-First International Joint Conference on Artificial Intelligence, IJCAI 2022, Vienna, Austria, 23-29 July 2022*, Luc De Raedt (Ed.). ijcai.org, 4995–5001. <https://doi.org/10.24963/IJCAI.2022/692>

A Dataset Examples

In this section, we provide examples from the PITA and PIL datasets, illustrated in Figures 8 and 9, respectively. The PITA dataset includes advertising images with marketing taglines. In addition to depicting the layout of both graphic and nongraphic elements as shown in the figures, we also label the image caption (prompt), tagline content, and product foreground masks to train the prompt and layout generation models. Conversely, the PIL dataset contains product images without taglines. We annotate the layout of nongraphic elements and product foreground masks for training the image generation model.



Figure 8: Examples from the PITA dataset, with tagline, underline, and logo highlighted in orange, yellow, and red rectangles, respectively.

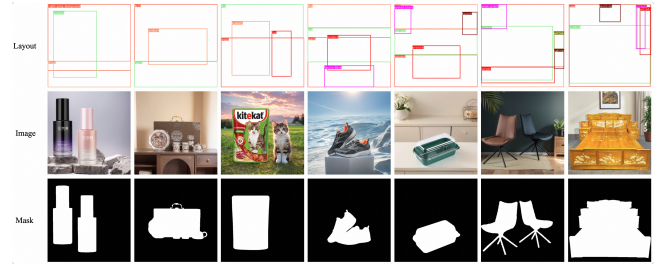


Figure 9: Examples in PIL dataset.

B Visualization of Prompt Distribution

We use t-SNE for dimensionality reduction to visualize the feature distribution of prompts generated by our model before and after training (see Figure 10). This shows that our model effectively aligns with the e-commerce prompt dataset distribution after training.

C Ablation Studies

To verify the effectiveness of our design, we conduct ablation studies on the methods and strategies used in each module.

C.1 Effect of JPGNL in Layout Generation

Our method predicts the overall layout of graphic and nongraphic elements. Here, we examine the need to predict the layout of nongraphic elements according to the background prompt. As shown in Figure 11, without specifying the position of nongraphic elements, taglines placed on complex areas can lead to a messy appearance. By predicting the overall layout, we improve the tagline readability

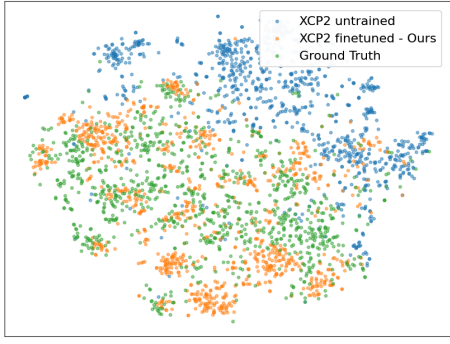


Figure 10: T-sne visualization of generated prompts.

of advertising images. Additionally, with nongraphic layout predictions, generated images align more closely with background prompts. Without JPGNL, images might miss some objects from the prompts. Besides, in Table 5, we quantitatively analyze the impact of predicting nongraphic layouts on graphic layouts. Predicting nongraphic layouts (w/ JPGNL) can improve metrics related to product occlusion and tagline readability. However, since it adds complexity to the task, it negatively affects graphic metrics such as element overlap and alignment.

Table 5: Quantitative ablation study on JPGNL.

Method	Val↑	Ove↓	Ali↓	Und _l ↑	Und _s ↑	Uti↑	Occ↓	Rea↓
w/o JPGNL	1.0	0.0009	0.0013	0.9995	0.9891	0.1377	0.1001	0.2003
w/ JPGNL	1.0	0.0012	0.0017	0.9976	0.9956	0.1364	0.0973	0.1968

C.2 Effect of RKBR and CCLP in Layout Generation

We validate the effectiveness of the proposed input and output format for layout generation, including RKBR and CCLP. As shown in Table 6, without RKBR, the model may predict a product size which does not match the original aspect ratio about 5% of the time. Note that we regard a difference of less than 1.5% as correctness. Adding CCLP improves the Uti and Occ values on No Occ Set, indicating that CCLP helps the model to distinguish occlusion-allowing sets and others by providing explicit class conditions.

Table 6: Ablation study on input/output format construction of layout generation. *O*, *NO*, and *AO* correspond to the overall set, the No Occ Set, and the Allow Occ Set, respectively. FRC represents Fg Ratio Correctness.

RKBR	CCLP	Val↑	Ove↓	Ali↓	Und _l ↑	Und _s ↑	Uti(O↑/NO↑/AO)	Occ(O↓/NO↓/AO)	Rea↓	FRC↑
✗	✗	1.0	0.0012	0.0018	0.9982	0.9971	0.1353/0.1448/0.0876	0.0985/0.0230/0.4258	0.2005	0.955
✓	✗	1.0	0.0012	0.0018	0.9991	0.9912	0.1360/0.1466/0.0816	0.1054/0.0209/0.4491	0.1994	1.0
✗	✓	1.0	0.0008	0.0018	0.9989	0.9906	0.1366 /0.1492/0.0851	0.1002/0.0156/0.4282	0.1973	0.957
✓	✓	1.0	0.0012	0.0017	0.9976	0.9956	0.1364/ 0.1493 /0.0849	0.0973 / 0.0136 /0.4316	0.1968	1.0



Figure 11: An illustration of the effect of JPGNL. Predicting image layout makes better visual effect.

C.3 Effect of DLC and LAT in Layout-to-Image Model

We investigate the effect of deep layer control (DLC) and Lora adaptation training (LAT), with results shown in Table 7. Adding layout control in deep UNet layers performs almost as well as controlling all layers. It reduces parameters and inference costs, which benefits the application. With LoRA adaptation, the model achieves lower FID and higher mIoU, enhancing image quality and spatial control. Parameters and inference costs can be further reduced.

Table 7: Quantitative performance comparison of layout-to-image methods on PIL dataset.

DLC	LAT	FID↓	CLIP-T↑	CLIP-I↑	mIoU↑	AP/AP50/AP75↑
✗	✗	27.237	0.312	0.898	0.561	0.047/0.073/0.044
✓	✗	27.308	0.312	0.898	0.558	0.045/0.075/0.043
✗	✓	25.675	0.313	0.906	0.696	0.076/0.123/0.075
✓	✓	25.917	0.313	0.906	0.705	0.079 /0.127/0.078